



Localization of Faults in 11KV/220KV/400KV Underground Cables by Wavelet Transform

D.Prabhavathi¹, Dr.M.Surya Kalavathi², K.Prakasam³

PhD Scholar, Department of EEE, JNTUA, Anantapur, A.P India¹

Professor, Department of EEE, JNTUCEH, JNTUH, Hyderabad, T.S, India²

PhD Scholar, Department of EEE, JNTUA, Anantapur, A.P, India³

ABSTRACT: This paper deals with localization of faults in 11kV, 220kV and 400kV underground power cables by wavelet Transform. In this research work a three - phase 11KV, 200kV and 400kV long XLPE cable has been considered and the simulation model of proposed system was prepared using Mat Lab software. The test simulation has been carried for LL Core to Core), LLL (Three core) and sheath faults at fault locations of 25Km and 50Km and the outcomes of the proposed system are explored to wavelet transform (Mexican Hat and Coif Let) for extraction of high frequency transient signals. The outcome of the results shows that the percentage error in location of faults is very less and wavelet method is found to be efficient and powerful to estimate the exact location of faults in three phase underground cables.

KEYWORDS: Cable, Extraction, Fault, Coif let, Mexican hat, Travelling, Transients.

I.INTRODUCTION

In electrical power systems, the underground cables plays an important and vital role in power distribution networks due to the benefits of underground connection, involving more secure than overhead lines in bad weather, less liable to damage by storms or lightning, no susceptible to trees, less expensive for shorter distance, environment-friendly and low maintenance. However, the disadvantages of underground cables should also be mentioned, including 8 to 15 times more expensive than equivalent overhead lines, less power transfer capability, more liable to permanent damage following a flash-over, and difficult to locate fault. On the basis of broad category, faults in underground cables can be normally classified as, incipient faults and permanent faults

Fault location based on the travelling waves can generally be categorized into two: single-ended and double ended. For single-ended, the current or voltage signals are measured at one end of the cable and fault location relies on the analysis of these signals to detect the reflections that occur between the measuring point and the fault. For the double-ended method, the time of arrival of the first fault generated signals are measured at both ends of the cables using synchronized timers. Detection and Location of faults in power cables are one of the main concerns for all the electric utilities as the accurate detection and fault location can help to restore the power supply in the shortest possible time. Fault location methods for power cables are broadly classified as impedance based method which uses the steady state fundamental components of voltage and current values, travelling wave (TW) based method which uses incident and reflected (TWs) observed at the measuring end(s) of the cable and Knowledge based method which uses artificial neural network and/or pattern recognition techniques.

All the above methods use the measured data either from one end of the cable or from all ends. Fault analysis methods are an important tool used by protection engineers to estimate power system currents and voltages during disturbances. It provides information for protection system setting, coordination and efficiency analysis studies. Today, three approaches are used in the industry for such analysis: classical symmetrical components, phase variable approach and complete time-domain simulations. Classical fault analysis of unbalanced power systems is based on symmetrical components approach. However, in transposed feeders with single-phase or double- phase laterals, the symmetrical component methods do not consider accurately these specific characteristics. Hence, symmetrical component based techniques may not provide accurate results for power distribution systems, which are normally characterized by those



International Journal of Advanced Research in Electrical, Electronics and Instrumentation Engineering

(An ISO 3297: 2007 Certified Organization)

Website: www.ijareeie.com

Vol. 6, Issue 2, February 2017

asymmetries. With industrial computer facilities improvement, the fault analysis phase variable approach has been proposed to substitute the symmetrical component's methods on distribution systems. In the phase variable approach, system voltages and currents are related through impedance and admittance matrices based on phase frame representation, considering the typical distribution systems asymmetries. However, fault analysis still depends on the fault resistance.

The literature includes, Din et.al [1] proposed a novel wavelet-based travelling wave based cable fault locator scheme, the developed wavelet processing has been applied on the modal coordinated instead of the phase coordinates and the developed system has been found to be capable of eliminating the effect of the change in the propagation velocity of the travelling waves that can be significant for solving the problem of cable changing parameters especially the changing of the relative permittivity of the cable over its age.

Prasanna et.al [2] presented a single-ended travelling wave -based fault location and distance protection method for a hybrid transmission line. Author has employed Bewley diagrams for the traveling wave patterns and the wavelet coefficients of the aerial mode voltage to locate the fault. Mousa et al [13] proposed a new fault location system based on the travelling wave principle which was found to be capable of locating faults on power lines to within one tower span (300 m). The authors through their work claimed that unlike earlier schemes which are based on impedance measurements, its accuracy is not affected by load conditions, high grounding resistance and most notably series capacitor banks. This system measures the time of arrival of a fault-generated travelling wave at the line terminals using the precise timing signals from the GPS. Operating experience with the fault locator on lightning related faults indicated highly accurate results were obtained for the majority of the cases. In a few of the lightning-caused disturbances, the system gave anomalous measurements.

Apisit et al [3] proposed a technique for identifying the phase with fault appearance in underground cable where they employed the wavelet transform to extract high frequency components superimposed on fault signals simulated using ATP/EMTP. The coefficients obtained from the Wavelet transform were used in constructing a decision algorithm.

Chiradeja et al [4] proposed a new technique using DWT and artificial neural network for fault classifications on single circuit transmission lines. Authors employed the mother wavelet Db4 to decompose, high frequency components. Positive sequence current signals then employed for fault detection decision algorithm. In their research work the variations of first scale high frequency component that detect fault were used as an input for the training pattern and the robust back-propagation (BP) neural network was also compared with the RBF neural network. The authors in their research stated that the average accuracy values achieved through RBF gives satisfactory results with less training time.

Youssef et.al [5] presented a new approach to real-time fault classification in power transmission systems using fuzzy-logic-based multi-criteria approach. They employed only the three line currents to detect fault types such as LG, LL, and LLG. Authors also employed the online wavelet-based pre-processor with data window of ten samples and developed a novel multi-criteria algorithm based on fuzzy sets for the decision-making part of the scheme.

NgaopitakKul et.al [6] developed a Wavelet Transform based on traveling wave to detect the high frequency components and to identify fault locations in the underground distribution system.

Long et.al [7] presented fault detection in underground power cables by examining voltage and current signals using signal processing techniques. The author explored the feasibility of complex wavelet analysis scheme for fault detection and combined the complex wavelets with CWT, and the impedance were calculated from the voltage and current data in the wavelet domain. Their results stated the fact that complex wavelet analysis based approach is able to provide unique signatures for distinguishing between the cables, thus very promising for fault detection.

Livani et al [8] proposed hybrid method, DWT was utilized to extract transient information of recorded voltages and later the SVM algorithm was employed to identify the section of the fault. The normalized wavelet energies of post-fault voltages were used as the input to the classifier. The author observed the Bewley diagrams for the traveling wave pattern in the overhead line and underground cable to locate the fault in the proposed system.

[9] Gilany, M.; Ibrahim, D.K.; Eldin, E.S.T., "Traveling-Wave-Based Fault-Location Scheme for Multiend-Aged Underground Cable System," Power Delivery, IEEE Transactions on, 22(1) (2007) 82- 89.

II. FAULTS IN UNDERGROUND CABLES

In general, there are three predominant types of faults in underground power cable; these are single phase-to-earth (LG) fault; double phase-to-earth (LLG) fault and three phase-to-earth (LLLG) fault. The single phase to earth fault is the most common fault type and occurs most frequently. Fault detection and location based on the fault induced current or

International Journal of Advanced Research in Electrical, Electronics and Instrumentation Engineering

(An ISO 3297: 2007 Certified Organization)

Website: www.ijareeie.com

Vol. 6, Issue 2, February 2017

voltage travelling waves has been studied for years together. In all these techniques, the location of the fault is determined using the high frequency transients. In general the faults in underground power cables can be divided into two types, Fault between core – core and /or core –sheath, low resistive faults ($R < 10\text{-}200\Omega$)- short circuit fault comes under this type, high resistive faults($R > 100\text{-}200\Omega$)-Intermittent faults (Breakdown or flash faults). Interruption faults defects on the outer protective shield- cable sheath fault, most of the cable faults occur between cable core and sheath furthermore, very frequently blown up open joint connections or vaporized cable sections can cause the core to be interrupted. To figure out whether r such faults present, the loop resistance test can be done and the loop resistance can be evaluated from the following equation (1).

$$R_L = \frac{\rho_c X l}{A_c} + \frac{\rho_s X l}{A_s} \quad (1)$$

ρ_c = spec core resistance,

for Al: $0.0178\Omega \text{ mm}^2/\text{Km}$,

ρ_s = spec sheath resistance,

for cu: $0.028 \Omega \text{ mm}^2/\text{Km}$,

A_c = cross sec of core or conductor - 185 mm^2 ,

A_s = cross sec of sheath- 35 mm^2

III.LOCALIZATION OF FAULTS

In this scheme, each node with message searches for possible path nodes to copy its message. Hence, possible path In this research work, initially the proposed system has been subjected to LL and LLL faults at 25Km and 50Km fault points and the outcomes were explore to wavelet transforms (Mexican Hat and Coif Let) to extract the high frequency signals[1, 2]. The fault performance has been evaluated in terms of % error and the deviation from the actual values. The overall process of fault detection and location has been accomplished as follows. Consider a three phase cable line of length X connected between bus A and bus B, with characteristic impedance Z_c and travelling wave velocity of v . The single line diagram of proposed system is shown in fig.1 and the overall flowchart of the proposed algorithm used for estimation of fault is shown in figure.2.

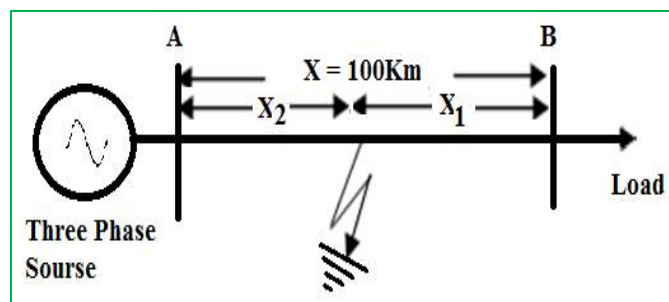


Fig .1 Single line diagram of proposed system

Fig.1 presents a three phase underground cable diagram with total length of 100Km, with fault point of X_2 from the source and X_1 from the load end.

International Journal of Advanced Research in Electrical, Electronics and Instrumentation Engineering

(An ISO 3297: 2007 Certified Organization)

Website: www.ijareeie.com

Vol. 6, Issue 2, February 2017

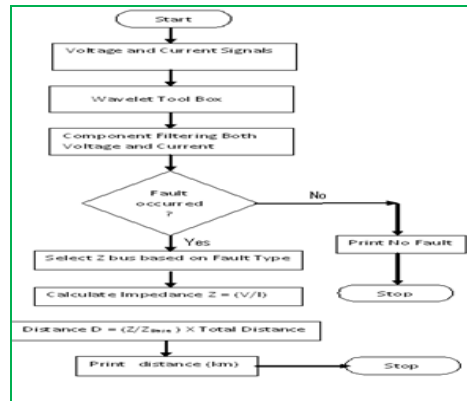


Fig .2The overall flowchart of the proposed algorithm

Fig. 2 presents the method of location of fault in the present study, in which initially, the voltage and current signals are captured and extracted to wavelet tool box and voltage and current signals are filtered then the comparison of fault condition existed to decide whether the fault occurred or not. Then the selection of Z_{bus} based on the base value and calculation of impedance done if fault is occurred. The fault distance has been estimated by the base impedance and actual impedance in multiplication of actual distance of the cable.

The flow chart of algorithm presents how the voltage and current signals used for estimation of fault location and application of wavelet tool box. Initially, both voltage and current signals are extracted and explored to wavelet transform filtering achieved for de-noising coefficients. Comparison of impedance done with without fault conditions as per the Z_{bus} predetermined. Initially, the proposed system has been simulated and travelling wave generated by the faults are captured [7] and the location of fault is estimated and it has been found that if a fault occurs at a distance X_2 from bus A, this will appear as an abrupt injection at the fault point. Let t_1 and t_2 corresponds to the times at which the first peak and second peaks recorded at bus A and bus B. the delay between the fault detection times at the two ends is $(t_1 - t_2)$ can be determined. Once the parameter t_d is determined, the fault location can be estimated as per the following expression (2).

$$D = \frac{v \times t_d}{2} \quad (2)$$

Once the parameter t_d is determined, the fault location X_2 from bus A can be estimated as per the following expression (3).

$$X_2 = X - \frac{(t_1 - t_2)v}{2} \quad (3)$$

Or the fault location X_1 can be calculated from bus B as follows expression (4)

$$X_1 = X - \frac{(t_2 - t_1)v}{2} \quad (4)$$

The travelling wave velocity can be obtained from the equation (5)

$$v = \frac{3 \times 10^8}{\sqrt{\epsilon_r \mu_r}} \text{ m/s} \quad (5)$$

Where,

μ_r is relative permeability of cable ($\mu_r = 1$) and ϵ_r is relative dielectric coefficient ($\epsilon_r = 2.7$). The velocity of propagation for 11kV, 220kV and 400kV cables can be assumed to be 87m/ μ s, 285 m/ μ s and 395 m/ μ s, respectively. Further, the high frequency transient signals are explored to the wavelet transform [2, 3, and 7] for extraction of transient signals and wavelet coefficients for exact fault location. In this analysis Mexican Hat and Coiflet transforms are employed for localization of fault.

IV.MAT LAB SIMULATION MODEL OF PROPOSED SYSTEM

The proposed systems (11KV, 220KV and 400KV) underground power cables has been selected and based on the mathematical model of the systems the simulation model has been prepared using Mat Lab software. The simulation model of the proposed system is shown in fig.3.

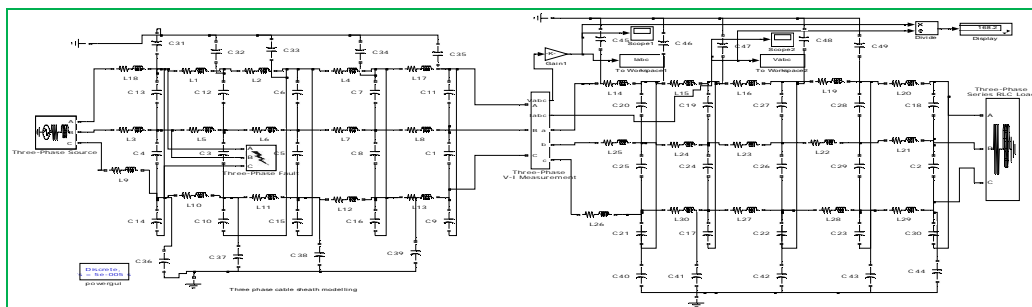


Fig. 3 Simulation model of proposed system

V. RESULT AND DISCUSSION

The simulation test for the proposed three – phase 11KV, 220KV ad 4000KV cable have been carried for LL and LLL faults at 25Km and 50Km fault locations and the fault current responses for both LL and LLL for faults at 25Km are accomplished in the following section from fig.3 to fig.19 in the following section. In the similar manner the simulation test for LL and LLL fault at 50Km location also carried and its outcomes tabulated in table 2. Fig.4 to fig.9 presents the simulation outcomes of 11KV for fault LL and LLL at 25m, fig.10 to fog.15 presents the simulation results of 220KV, for LL and LLL fault at 25Km and fig.12 tofig.15 presents results of 220KV, for LL and LLL faults at 25Km and fig.16 to fig.21presents the outcomes of 400KV, LL and LLL fault at 25Km. Similarly the test simulation has been carried for 50Km fault point and the retrieved outcomes of the simulation carried have been accomplished in table 1.

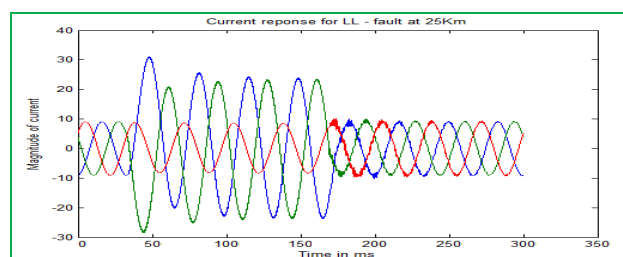


Fig. 4 current response for LL - fault at 25Km

The fig.4 shows the graph of time Vs magnitude of current and it presents current response for 11KV, LL – fault at 25Km and from which it can be observed that there is a rise of fault current for phase A and phase B about 31.42A and 20.17A respectively.

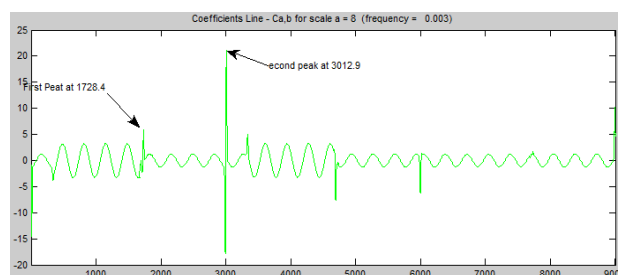


Fig. 5 Current response for LL - fault at 25Km Mexican Hat

International Journal of Advanced Research in Electrical, Electronics and Instrumentation Engineering

(An ISO 3297: 2007 Certified Organization)

Website: www.ijareeie.com

Vol. 6, Issue 2, February 2017

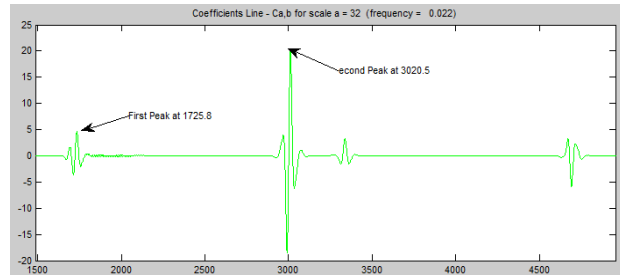


Fig .6 Current response for LL - fault at 25Km Coif Let

The fig.5 and fig.6 presents the fault current response for LL fault at 25Km by Mexican Hat and Coif Let, the first peak and second peaks occurs at 1728.4 and 3009.7 with Mexican hat and it is 1725.8 and 3020.5 with Coif Let.

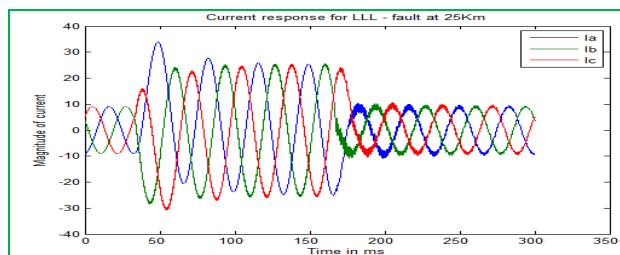


Fig .7 Current response for LLL - fault at 25Km

The fig.7 shows the graph of time Vs magnitude of current and it presents current response for 11KV, LLL – fault at 25Km and from which it can be observed that there is a rise of fault current for phase A and phase B about 36.47A and 24.17A respectively.

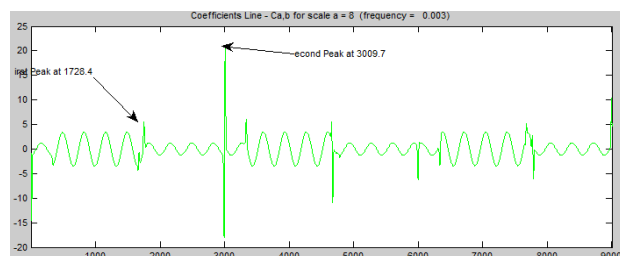


Fig .8 Current response for LL - fault at 25Km Mexican Hat

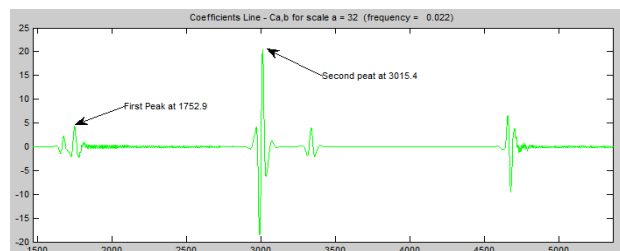


Fig .9 Current response for LLL - fault at 25Km Coif Let

The fig.8 and fig.9 presents the fault current response for LLL fault at 25Km by Mexican Hat and Coif Let, the first peak and second peaks occurs at 1728.4 and 3009.7 with Mexican hat and it is 1725.9 and 3015.4 with Coif Let.

International Journal of Advanced Research in Electrical, Electronics and Instrumentation Engineering

(An ISO 3297: 2007 Certified Organization)

Website: www.ijareeie.com

Vol. 6, Issue 2, February 2017

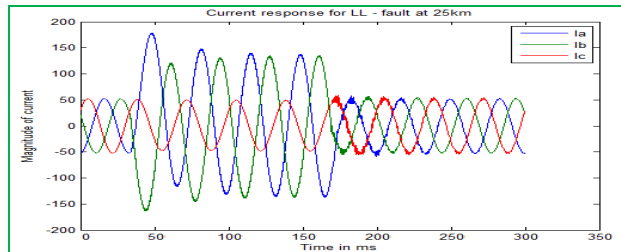


Fig .10 Current response for LL - fault at 25Km

The fig.10 shows the graph of time Vs magnitude of current and it presents current response for 220KV, LL – fault at 25Km and from which it can be observed that there is a rise of fault current for phase A and phase B about 179.85A and 122.34A respectively.

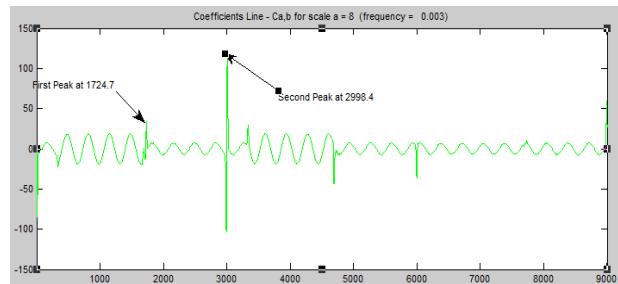


Fig.11 current response for LL - fault at 25Km Mexican Hat

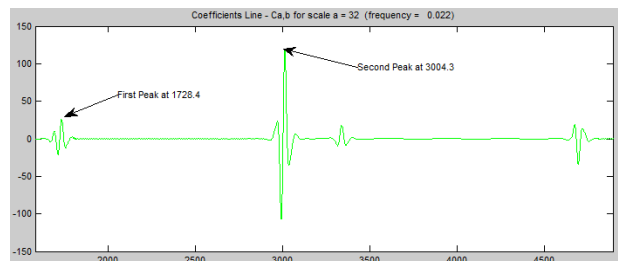


Fig .12 Current response for LL - fault at 25Km Coif Let

The fig.11 and fig.12 presents the fault current response for LL fault at 25Km by Mexican Hat and Coif Let, the first peak and second peaks occurs at 1724.7 and 2998.4 with Mexican hat and it is 11728.4 and 3004.3with Coif Let.

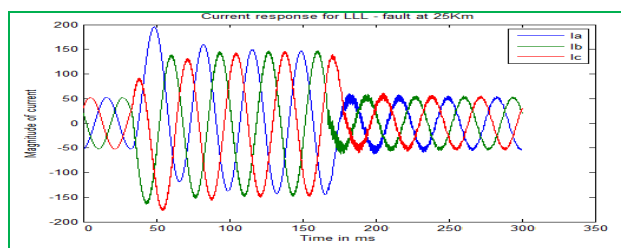


Fig .13 Current response for LLL - fault at 25Km

The fig.13 shows the graph of time Vs magnitude of current and it presents current response for 220KV, LLL – fault at 25Km and from which it can be observed that there is a rise of fault current for phase A and phase B about 200A and 147.85A respectively.

International Journal of Advanced Research in Electrical, Electronics and Instrumentation Engineering

(An ISO 3297: 2007 Certified Organization)

Website: www.ijareeie.com

Vol. 6, Issue 2, February 2017

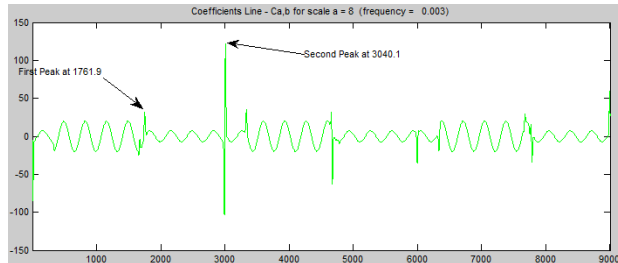


Fig .14 Current response for LLL - fault at 25Km Mexican Hat

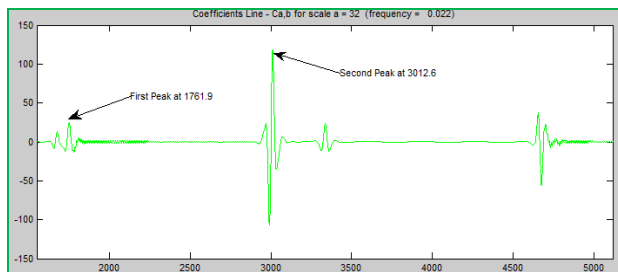


Fig .15 Current response for LLL - fault at 25Km Coif Let

The fig.14 and fig.15 presents the fault current response for LLL fault at 25Km by Mexican Hat and Coif Let, the first peak and second peaks occurs at 1761.9 and 3040.1 with Mexican hat and it is 1761.9 and 3012.8with Coif Let.

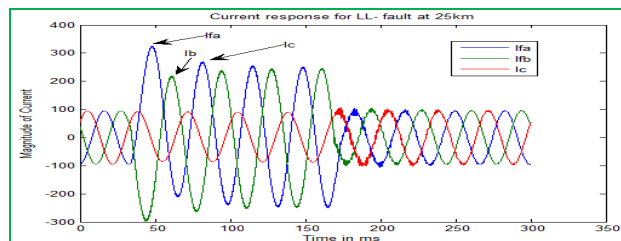


Fig .16 current response for LL - fault at 25Km

The fig.16 shows the graph of time Vs magnitude of current and it presents current response for 400KV, LL – fault at 25Km and from which it can be observed that there is a rise of fault current for phase A and phase B about 312.25A and 215.65A respectively.

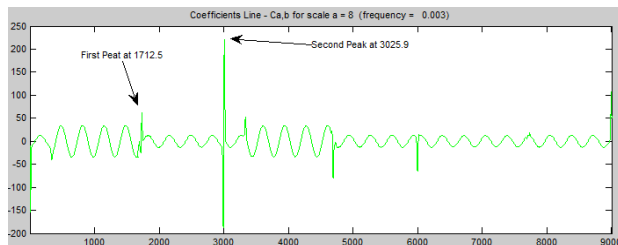


Fig .17 Current response for LL - fault at 25Km Mexican Hat

International Journal of Advanced Research in Electrical, Electronics and Instrumentation Engineering

(An ISO 3297: 2007 Certified Organization)

Website: www.ijareeie.com

Vol. 6, Issue 2, February 2017

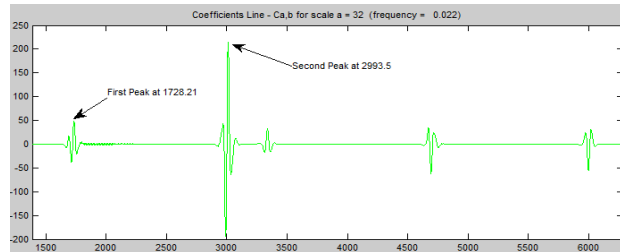


Fig .18 Current response for LL - fault at 25Km Coif Let

The fig.17 and fig.18 presents the fault current response for LLL fault at 25Km by Mexican Hat and Coif Let, the first peak and second peaks occurs at 1712.5 and 3025.9 with Mexican hat and it is 1728.21 and 2993.5 with Coif Let.

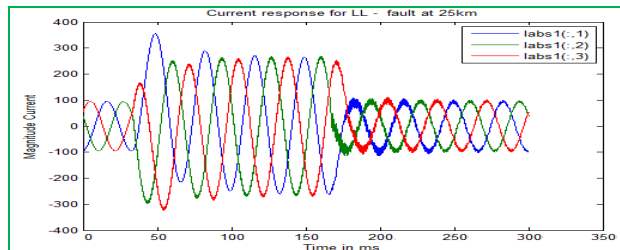


Fig .19 Current response for LLL - fault at 25Km

The fig.19 shows the graph of time Vs magnitude of current and it presents current response for 400KV, LLL – fault at 25Km and from which it can be observed that there is a rise of fault current for phase A and phase B about 364.56A and 257.95A respectively.

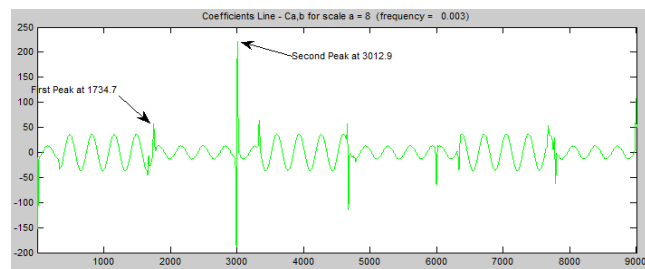


Fig .20 Current response for LLL - fault at 25Km Mexican Hat

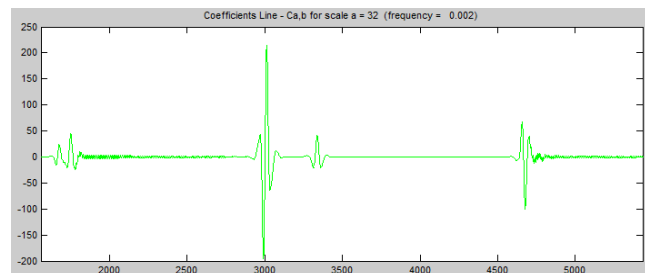


Fig .21 Current response for LLL - fault at 25Km Coif Let

The fig.20 and fig.21 presents the fault current response for LLL fault at 25Km by Mexican Hat and Coif Let, the first peak and second peaks occurs at 1734.7 and 3012.9 with Mexican hat and it is 1715.9 and 3015.6 with Coif Let.



International Journal of Advanced Research in Electrical, Electronics and Instrumentation Engineering

(An ISO 3297: 2007 Certified Organization)

Website: www.ijareeie.com

Vol. 6, Issue 2, February 2017

Table 1 Percentage Error Estimated by Proposed Methods

| Three phase Cable Voltage | 11kV | | 220kV | | 400kV | |
|---|-------|-------|-------|-------|-------|-------|
| Fault Type | LL | LLL | LL | LLL | LL | LLL |
| Actual Distance (Km) | 25 | 50 | 25 | 50 | 25 | 50 |
| Estimated Distance (Km) Impedance method | 26.24 | 49.54 | 26.62 | 52.49 | 26.78 | 52.79 |
| % Error by Impedance Method | 1.24 | 1.54 | 1.62 | 2.49 | 1.78 | 2.79 |
| by Mexican Hat | 25.21 | 50.21 | 25.27 | 50.22 | 25.37 | 50.42 |
| Estimated by Coif Let | 25.12 | 50.14 | 25.15 | 50.16 | 25.12 | 50.27 |
| % Error by Mexican Hat | 0.21 | 0.21 | 0.27 | 0.22 | 0.37 | 0.42 |
| % Error by Coif Let | 0.12 | 0.14 | 0.15 | 0.16 | 0.12 | 0.24 |

VI.CONCLUSION

The proposed systems (11kV, 220kV and 40k0V) have been subjected to LL and LLL faults and the fault locations were estimated for 25Km and 50Km fault points initially, by travelling wave method and the fault location measured and then the Mexican hat and Coif Let wavelet transform techniques employed for extraction of high frequency transient signals. The retrieved percentage error in fault location has been tabulated in table1. From the outcomes the following are noted.

For a fault at 25Km & Km in 11kV cable, the measured value by impedance method is 26.24Km for LL and it is 49.54Km respectively, whereas by Mexican hat it is 25.21Km and 50.21Km and by Coif Let method it is 25.12Km and 50.14Km respectively. From this it is very clearly can be decided that the percentage error by Coif Let is very small and little more it is by Mexican Hat , however when compared to impedance method both Mexican Hat and Coif Let wavelet Transforms are more better and they gives almost exact fault location. The same results repeated for 220kV and 400kV cases also which have been tabulated in table 1.

The percentage error is very high in case of impedance method and it is very less in case of Mexican hat wavelet transform (WT- Mexican Hat and Coif Let).

Finally, it can be stated that the wavelet transform technique is more powerful tool for localization of faults in underground cables since it gives exact location of fault.

REFERENCES

- [1] Din, E.S.T.E.; Gilany, M.; Abdel Aziz, M.M.; Ibrahim, D.K., "A wavelet-based fault location technique for aged power cables," Power Engineering Society General Meeting, IEEE, 3, pp. 2485- 2491, 12-16, 2005.
- [2] K. Prasanna Kumar, K. Durga Syam Prasad, K. Sravanthi "Wavelet-Based Fault Location and Distance Protection Method for Transmission Lines" Int. Journal of Engineering Research and Applications, vol. 7, pp. 05-16, 2014.
- [3] C. Apisit and A. NgaopitaKKul, "Identification of Fault Types for Underground Cable using Discrete Wavelet transform", Lecture Notes in Engineering and Computer Science: Proceedings of The International MultiConference of Engineers and Computer Scientists pp. 1262-1266, 2010.
- [4] P. Chiradeja and A. NgaopitaKKul, "Identification of Fault Types for Single Circuit Transmission Line using Discrete Wavelet Transforms and Artificial Neural NetworKs", The International Multi-Conference of Engineers and Computer Scientists , pp. 21520-1525, 2009.
- [5] A. K. Pradhan, A. Routray, S. Pati and D. K. Pradhan, "Wavelet Fuzzy Combined Approach for Fault Classification of a Series-compensated Transmission Line", IEEE Trans. On Power Delivery, vol. 19 no. 4, pp. 1612-1618, 2004.



ISSN (Print) : 2320 – 3765
ISSN (Online): 2278 – 8875

International Journal of Advanced Research in Electrical, Electronics and Instrumentation Engineering

(An ISO 3297: 2007 Certified Organization)

Website: www.ijareeie.com

Vol. 6, Issue 2, February 2017

- [6] A. NgaopitaKKul, C. Apisit, C. Pothisarn, C. Jettanasen and S. JaiKhan "Identification of Fault Locations in Underground Distribution System using Discrete Wavelet Transform" Proceedings of the International MultiConference of Engineers and Computer Scientists 2010 Vol II, IMECS, pp. 17 – 19, 2010.
- [7] Zhiling Long; Younan, N.H.; BialeK, T.O., "Underground power cable fault detection using complex wavelet analysis," High Voltage Engineering and Application (ICHVE), 2012 International Conference on ,vol. 59, pp. 17-20, 2012.
- [8] NgaopitaKKul, A.; Pothisarn, C.; LeelajindaKrairerK, M., "Study of characteristics for simultaneous faults in distribution underground cable using DWT," TENCON IEEE Region 10 Conference, pp. 21-24. 2011.
- [9] Gilany, M.; Ibrahim, D.K.; Eldin, E.S.T., "Traveling-Wave-Based Fault-Location Scheme for Multiend-Aged Underground Cable System," Power Delivery, IEEE Transactions on, vol. 22, pp. 82- 89, 2007.